

Temperature dependence and anisotropy of charge carrier mobilities in durene

Z. Burshtein and D. F. Williams

Division of Chemistry, National Research Council of Canada, Ottawa, Canada K1A 0R6

(Received 27 December 1976)

Very high charge-carrier drift mobilities have been measured in durene (1,2,4,5 tetramethyl benzene) single crystals by the transient-photoconductivity technique. In the crystal (*a, b*) plane both hole and electron mobilities are isotropic, 5 cm²/V sec and 8 cm²/V sec, respectively, at room temperature, and follow a $T^{-2.5}$ temperature dependence. In the *c'* direction only hole mobilities could be measured, which were 0.15 cm²/V sec at room temperature and followed a $T^{-2.8}$ temperature dependence. These results indicate that charge-carrier transport in durene can be treated within the frame of the band model. The charge-carrier generation process for the excitation wavelength (nitrogen laser $\lambda = 3371 \text{ \AA}$) was also studied. It is shown that the process involves a direct two-photon absorption to produce singlet excitons which then dissociate at surface states giving charge carriers. A lower limit of $\sim 10^{-48} \text{ cm}^4 \text{ sec}/(\text{photon molecule})$ was estimated for the molecular singlet-singlet excitation-rate constant.

I. INTRODUCTION

Interest in the electronic properties of organic materials has steadily increased since the first suggestion by Szent-Györgyi¹ in 1941 that macromolecules may play a role in electron-transfer reactions of biological importance. The latest impetus has been given by Heeger and co-workers² who found that the conductivity of certain charge-transfer materials, predominantly tetracyanoquinodimethane salts, showed a sharp maximum at low temperatures which, perhaps, could have been ascribed to a certain mode of superconductivity. Unfortunately, although much of the theoretical interest has been to provide a proper description of the transport properties of these materials, an unequivocal answer has not yet been obtained, particularly in the case of molecular crystals. The essential difference between a typical semiconductor and a molecular crystal lies in the relative magnitudes of their electron-exchange and electron-phonon interactions. Electron-exchange interactions are far more important than electron-phonon interactions for semiconductors. In molecular crystals, however, the electron-exchange interactions are much weaker, hence their charge-carrier mobilities are lower. Electron-phonon interactions are of the same magnitude for semiconductors and molecular crystals. Theoretically and experimentally the most extensively studied molecular crystals are the polyacenes: naphthalene and anthracene. For anthracene the electron mobility in the crystallographic *a, b* plane was found to decrease with increasing temperature, but perpendicular to this plane, *c'* direction, mobility increased slightly with temperature. Many theoretical attempts to

explain this behavior have been made,³ in general based on a conventional band-structure calculation with modifications to account for the mobility in the *c'* direction. Unfortunately, mean free paths calculated from this model approach the molecular lattice spacing, and the applicability of a band model becomes tenuous. Indeed some quantitative treatments of the electron-phonon coupling in aromatic hydrocarbons^{4,5} have concluded that electron-phonon coupling is of far greater importance than electron-exchange interactions in anthracene. The question whether in molecular crystals the electron-phonon interaction really can be treated as a small perturbation to the electron Bloch-type wave function is still in doubt.

In order to give further insight into this question of carrier transport in molecular crystals, we have started to study a series of crystals with the same basic crystallographic structure as anthracene, monoclinic with two molecules per unit cell, in which the electron-exchange interactions are increased (or decreased) by chemical substitution around or in the aromatic ring. One of our first choices was durene, 1, 2, 4, 5 tetramethyl benzene, in which the influence of the CH₃ substitution is not negligible. For example the singlet $\pi-\pi^*$ absorption frequency is shifted 1600 cm⁻¹ to the red in the vapor phase⁶ when compared to benzene, 38 089–36 488 cm⁻¹. Furthermore the crystal structure and phonon spectrum of durene are known, as well as successful methods for purification.

Durene shares with the polyacenes an important characteristic, namely, they are insulators, usually with band gaps in excess of 4.0 eV, and conduct electricity only if the charge carriers are produced by some extrinsic mechanism. In the

present study the charge carriers were produced by a light pulse from a nitrogen laser. The pulsed photoconductivity technique is very useful for the study of charge-carrier transport and trapping, as well as for the study of charge-carrier generation processes.

This work is divided into two parts. Section III A describes the charge-carrier transport properties of durene and Sec. III B the charge-carrier generation processes.

II. EXPERIMENTAL

The measurements were made on durene crystals grown from the melt by the Bridgman method. The starting material was purified by zone refining in an inert atmosphere for about 100 zone passes. Samples, typically $5 \times 5 \times 1$ mm, were cut by a wire saw and then polished on ethanol-soaked filter paper. Samples with thicknesses ranging from 0.4 to 2 mm were used. Crystallographic alignment of the samples was performed by standard x-ray techniques.

A pulsed nitrogen laser which provided short light pulses (12–15 nsec) of wavelength⁷ 3371 Å and integrated intensity of $\sim 10^{-3}$ J was used for the charge-carrier generation. The generation of charge carriers involves a two-photon process, for the first excited singlet state of crystalline durene⁸ lies at 2900 Å. This charge generation process is discussed later in detail. The sample was sandwiched between a transparent conducting glass which served as a front electrode, and a brass plate mounted on soft springs which acted as the back electrode. The light pulse could be focused on the sample either from the side or through the conducting glass. The crystal holder was mounted in a liquid-nitrogen Dewar. The temperature of the sample could be varied by changing the amount of liquid nitrogen contained in the Dewar. The crystal temperature was monitored by a copper-Constantan thermocouple. The high voltage across the sample was provided by a 410B Fluke high-voltage power supply. Upon excitation with the laser pulse, as the current flowed into the crystal, a parallel voltage was developed over a series resistor. This voltage was fed into a current amplifier, whose output was displayed on an oscilloscope screen and photographed on polaroid film. The oscilloscope and the nitrogen laser were triggered with a 214 A Hewlett-Packard pulse-generator. By changing the series resistance, either the current transient, or the integrated current transient could be observed. For anthracene crystals, each method gave mobilities equal to literature values.

III. RESULTS AND DISCUSSION

A. Charge-carrier mobilities

Figure 1 shows some typical transients which appear when the laser light pulse is focused onto the crystal. In this case the crystal was illuminated through the front conducting glass electrode which was positively biased. The upper part of the figure was obtained with a series resistor of 22 kΩ, the lower part with a series resistor of 10 MΩ. The latter obviously represents the integration of the former. Both types of signal-recording methods reveal the characteristics expected for charge-carrier generation in a narrow region close to the sample surface, where the generation time is short compared to the transit time. The sharp kink by which the current ends (upper part) or the voltage reaches its maximum value (lower part) marks the transit time t_t of the charge carriers through the sample which is given by⁹

$$t_t = L^2 / \mu V, \quad (1)$$

where L is the sample's thickness, V the voltage between the electrodes, and μ the effective drift mobility. The term "effective" stands for the case when the electric field does not coincide with one of the principal axes of the mobility tensor, hence the current flow and the field direction may be different, so that the current path is actually larger than L . The charge carriers, which give rise to

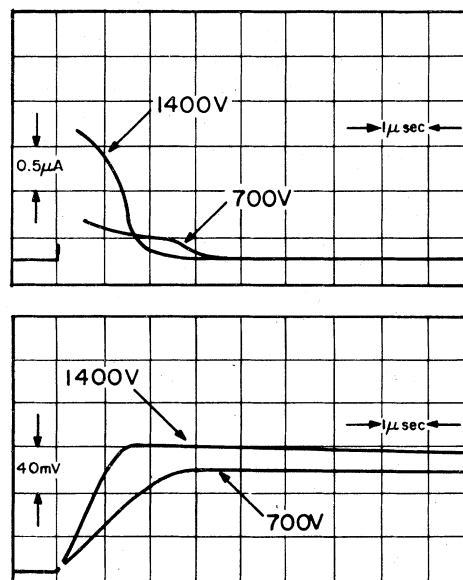


FIG. 1. Typical hole transients recorded for a series resistor of (i) 22 kΩ (upper part) and (ii) of 10 MΩ (lower part). Crystal thickness 1.25 mm. Field direction is 35° off the a, b plane, positive polarity to front electrode. Illuminated area ~ 1 mm², temperature 208 °K.

the curves shown in Fig. 1 are holes. This was confirmed by illumination of the front electrode through the side of the sample. Such experiments were necessary to establish which type of charge carrier was involved, for the crystal is almost transparent to the 3371-Å exciting light. The first strong optical transition in durene crystals⁹ occurs at ~ 2900 Å. The shape of the transients seen in Fig. 1 suggests that the charge-carriers are being produced at a crystal surface. However, with excitation parallel to the current path with weakly absorbed light, either holes produced at one electrode or electrons at the other electrode could give rise to the transients. With illumination of only one electrode it was possible to distinguish between transients of holes or electrons by simply reversing the polarity of the applied potential, and Fig. 1 indeed shows transient hole currents. The yield for free-electron production was always at least five times smaller than for holes, and for some sample surfaces, only holes could be measured.

For experimental convenience we preferred to measure the transit times of the charge carriers with the integrated current technique (large series resistor) for both the signal measured is larger, and of greater importance, the total collected charge is conveniently recorded in the same experiment. The collected charge Q is given by the product $C\delta V$, where C is the capacitance of the sample and connecting wires, and δV is the maximum voltage signal recorded. The capacitance C can be estimated from the long RC decay time of the signal where R is the series resistance. A typical value for C is 12 pF. The charge transferred by the currents was always much below the space-charge limitations. The trapping times in the samples studied were always longer than about 20–30 μ sec so that shorter transit times could be resolved fairly accurately.

The expected decrease of the transit time with

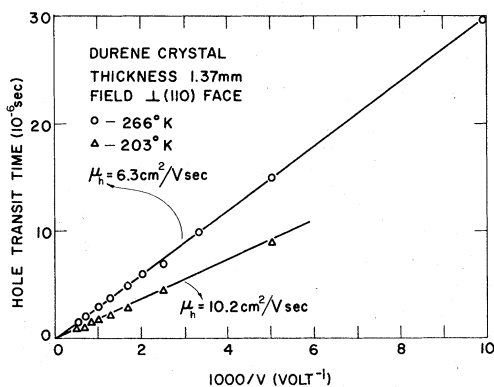


FIG. 2. Variation of the hole transit time as function of $1000/V$.

increasing voltage [Eq. (1)] is apparent in Fig. 1. A more detailed analysis of the voltage dependence is given in Fig. 2. Here, the hole transit time is plotted as a function of $1000/V$ for two different temperatures. As expected from Eq. (1) the experimental points lie on straight lines intersecting the origin. The effect of the change of the sample thickness on the transit time was also checked and was found to follow the square dependence of Eq. (1). As seen from Fig. 2, the effect of the temperature decrease is to increase the mobility. The temperature dependence for both holes and electrons was measured in various crystallographic directions¹⁰ in the range 100–300 °K. These results are shown in Fig. 3. Here the mobility vs temperature curves are plotted on a log-log scale. For the electric field \vec{E} in the a, b plane the mobilities of both holes (μ_h) and electrons (μ_e) were found to be isotropic and proportional to $T^{-2.5}$. The electron mobility is about 1.5 times larger than the hole mobility. For the direction perpendicular to the a, b plane (c' direction) only holes could be observed. Room-temperature hole mobilities were about 40 times smaller than in the a, b plane, and followed a $T^{-2.8}$ dependence.

The features of the carrier mobilities in durene are quite unique in view of the data accumulated so far on charge-carrier mobility in organic crystals,^{11–23} especially for its large values. We

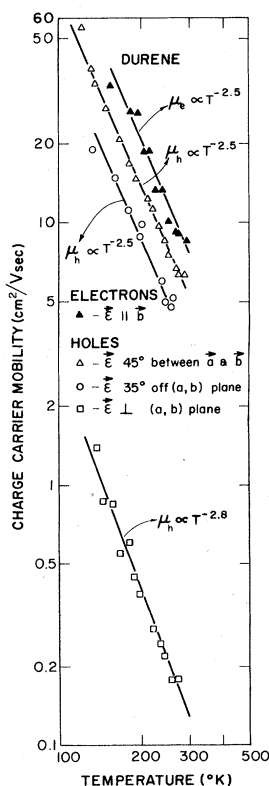


FIG. 3. Log-log plots of electron and hole mobilities in durene vs temperature for different crystallographic directions.

shall discuss first the anisotropy that is observed for holes. This anisotropy could be anticipated from the crystal molecular packing. The durene crystal is monoclinic with two molecules per unit cell.¹⁰ The unit cell dimensions are specified in Fig. 4(a). In Fig. 4(b) is shown the projection of the molecular arrangement along the c direction. The centers of all the molecules shown lie in the a, b plane, and the crystal is made up from such layers mounted one on top of another along the c direction. A small electronic overlap along the c' direction (compared to the a and b directions) is expected for two reasons: (a) the molecular planes are almost perpendicular (84°) to the crystal a, b plane, therefore the π orbital electronic wave functions overlap is small in the c' direction; (b) the intermolecular separation in the c' crystallographic direction is greater than in the a, b plane. Within the a, b plane, the shortest distance between the methyl groups on the standard and reflected molecules [denoted S and R , respectively, in Fig. 4(b)] is 3.93 \AA , and between adjacent molecules in the b axis is 3.87 \AA . On the other hand, along the c direction, the distance

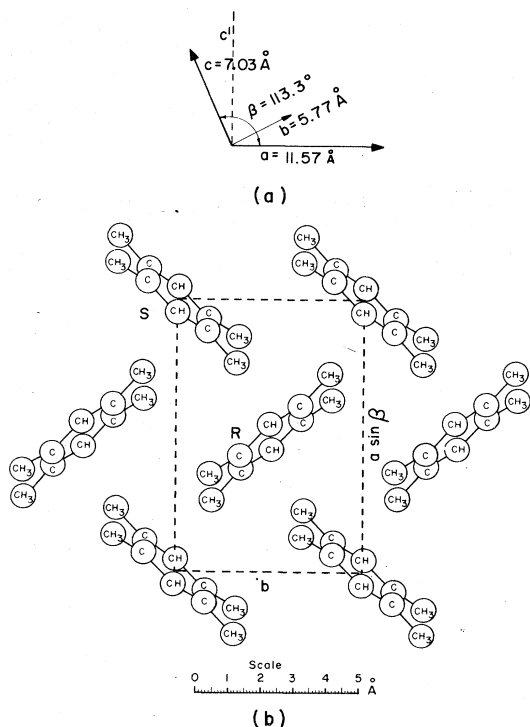


FIG. 4. (a) Unit cell dimensions of durene crystal. (b) Projection of molecular arrangement in the durene crystal along the c direction. The circles which represent the atoms are half size in each case. The letters S and R denote the standard and reflected molecules, respectively, which together constitute the pair of molecules attached to each lattice point to form the crystal.

between the methyl groups on adjacent molecules is 4.22 \AA , and between the standard and reflected molecule on translation along the c axis it is 4.15 \AA . These crystallographic features also influence the mechanical properties of the crystal; for example, the a, b plane is the most pronounced cleavage plane. In addition one should bear in mind the electronegativity of the methyl groups²⁴ which tends to push the π electron cloud towards the core of the molecule. This will further reduce the electronic overlap through the molecular edges. The fact that the hole mobility anisotropy reflects the expected anisotropy of the intermolecular electronic overlap is consistent with an isotropic hole scattering time.

The very high room-temperature mobilities, $\sim 5 \text{ cm}^2/\text{V sec}$, measured for durene in the a, b plane are unusual in the frame of the mobilities measured on organic crystals.¹¹⁻²³ To the best of our knowledge, there is only one case,²³ p -diiodobenzene, in which room-temperature drift mobilities as high as $\sim 10 \text{ cm}^2/\text{V sec}$ were reported. The largest room-temperature mobilities otherwise^{11, 20-22} are at $\sim 1-3 \text{ cm}^2/\text{V sec}$. In many cases mobilities as low as $10^{-1}-10^{-4} \text{ cm}^2/\text{V sec}$ were reported. Theoretically, two possible mechanisms for charge-carrier transport have been considered^{11, 25}; the band model or the small-polaron-hopping model. For the band model to be a good representation one needs that electron-phonon coupling be small compared to intermolecular electron coupling. In other words, the mean free path of the charge carrier should be long compared to the lattice period, so that it can be represented in a delocalized manner. For organic crystals it is expected that the charge-carrier bandwidth would be comparable to the room-temperature thermal energy $k_B T$, where k_B is Boltzmann's constant and T is the absolute temperature. For such a case and for a typical intermolecular separation of $\sim 3 \text{ \AA}$ it was estimated²⁶ that the mobility must exceed a value of about $1 \text{ cm}^2/\text{V sec}$. For mobilities much lower the small-polaron-hopping model should be applicable.

As already mentioned, except for one case with an exceptionally high room-temperature mobility,²³ the highest room-temperature mobilities reported^{11, 20-22} fall very close to the critical value of $1 \text{ cm}^2/\text{V sec}$ mentioned above. However, the temperature dependences suggest that the band model is correct. The mobilities generally follow a T^{-n} proportionality, where $1 < n < 2.5$, and this is expected where the dominant scattering mechanism of the moving charge carrier is its interaction with the crystal vibrations. Reducing the temperature results in a reduced phonon population, less scattering, thus an increase of mobility. The

actual value of n depends on the particulars of the band structure and the phonon spectrum. For isotropic bands and for scattering by acoustic lattice vibrations, a T^{-2} temperature dependence is expected.²⁷ If the electronic bands are narrow compared to the acoustic frequency band, the dominant scattering mechanism might involve a two-phonon process (i.e., the simultaneous absorption of one phonon and the emission of another). In that case one would expect a T^{-3} temperature dependence.²⁸ Anthracene, for which the most detailed studies have been performed, is considered an intermediate case.²⁹ This is due to the almost lack of temperature dependence for the electron mobility in the c' crystallographic direction.³⁰ In view of the similarity of the crystal structures of anthracene³¹ and durene¹⁰ (both being monoclinic with two molecules per unit cell, the space group is $P_{1/a}^2$) it would be worthwhile to compare published criteria for the validity of the band model for those two materials.^{26, 28}

The crystal structure is assumed to be cubic, with one molecule per unit cell. The bandwidth is assumed to be narrower than $k_B T$, but wider than the acoustic phonon band. It was then deduced²⁶ that the band model would be valid when the mobilities exceed a certain critical value μ_c given by

$$\mu_c \simeq (ea^2/\hbar)(\hbar\omega_0/k_B T), \quad (2)$$

where e is the electronic charge, a is the lattice period, \hbar is Planck's constant, and ω_0 the Debye frequency for acoustic waves. For electronic bands narrower than $\hbar\omega_0$, the bandwidth, rather than $\hbar\omega_0$ should appear²⁸ in Eq. (2). In order to generalize Eq. (2) for a monoclinic crystal with two molecules per unit cell, a should represent some average of the intermolecular distances, and ω_0 , the Debye frequency for the optical phonon waves. Compared to anthracene,³¹ the durene unit-cell dimensions¹⁰ are somewhat smaller, and ω_0 also is about a factor of two smaller.³²

The critical mobility μ_c for durene should thus be at least half of that for anthracene. One may take the experimental value of the electron mobility in the c' direction of anthracene, $0.4 \text{ cm}^2/\text{V sec}$, as a rough estimate for μ_c in that crystal. The value for the critical mobility for durene would thus be $\mu_c \sim 0.2 \text{ cm}^2/\text{V sec}$. The actual room-temperature hole and electron mobilities measured in the a, b plane of durene are thus more than an order of magnitude above the critical mobility. Even accepting the crude model which has been used in developing Eq. (2), it appears that the band model is a realistic model for carrier transport in durene. A mobility temperature dependence such as obtained in the a, b plane ($T^{-2.5}$), can therefore be rationalized. As for the c' direction, though the

room-temperature hole mobility is very close to the estimated critical value of $\sim 0.2 \text{ cm}^2/\text{V sec}$ (Fig. 3), the holes are still delocalized in view of the large mobilities in the a, b plane. One thus expects a very similar temperature dependence in all crystal directions, as found experimentally. Changes in crystal parameters are also reflected in these charge-carrier temperature dependences. For example, decreasing temperature decreases intermolecular distances, resulting in an increase for the electronic overlap between molecules. Also for the optical-phonon frequencies measured for durene,³² reducing the temperature results in a shift toward higher frequencies, particularly for the c' direction. This effect could be correlated to the higher power obtained for the temperature dependence of the hole mobility in the c' direction.

At present, there are no predictions based on either theoretical calculations or experimental results for the actual bandwidths for holes and electrons in durene. Therefore, whether the high mobilities in the a, b plane of durene are due to a larger electronic overlap (compared, say, to anthracene) or to a smaller electron-phonon scattering rate is open to question. Still, the high power for the temperature dependence might suggest that the electronic bands in durene are narrow so that only scattering by two phonons is possible, as suggested by Fröhlich and Sewell.²⁸ We are presently involved in band-structure calculations, which should help to clarify this point.

B. Charge-carrier generation

As mentioned earlier durene is transparent to the 3371-\AA exciting light. How the charge carriers are generated is thus not a trivial matter. The following experiments were performed to cast some light on the problem. Figure 5 shows the light-intensity dependence of the collected charge for hole generation. The slope of the straight line drawn through the points is 1.9, i.e., an almost square dependence of the amount of collected charge on the light intensity. Similar light-intensity dependencies were obtained for the various crystal directions studied, independent of voltage, temperature, or the type of charge-carrier produced. We interpret the deviation from a perfect square law to the recombination of charge carriers. This is considered later in more detail. Thus, carrier generation involves either a two-photon, or a bimolecular process. On considering the different possibilities one should remember that charge-generation takes place at the surface, in a process which lasts for $0.1 \mu \text{ sec}$ at most. These features are shown by the shape and resolution of the carrier transit times. The most ob-

vious process would be the interaction of photo-generated singlet excitons with surface states, for in anthracene crystals this is an efficient method for producing charge carriers.¹¹ The singlet excitons must be produced by either (i) bimolecular annihilation of triplet excitons which are themselves produced inefficiently by direct singlet \rightarrow triplet absorption,³³ or (ii) direct two-photon absorption.⁸ Process (i) is ruled out since the charge-carrier-generation process would reflect the long lifetime of the triplet excitons.³⁴ Other processes such as singlet-triplet or singlet-singlet annihilation can be excluded since they would imply bulk generation or show an incorrect light-intensity dependence. Direct two-photon transitions between the bands may just be energetically possible; the band gap is estimated³⁵ as 7.3 eV, but that would be a bulk generation process. In Fig. 6 we illustrate a possible process for the generation of a free electron at the crystal surface. A vibrationally excited singlet state S_x is produced in the crystal bulk via a two-photon absorption process. S_x rapidly decays to the first excited singlet electronic state S_0 , of energy E_s above the ground state. The singlet S_0 is phenomenologically described in Fig. 6 as a bound electron-hole pair state by full and open circles, respectively. It then diffuses to the surface of the crystal. The expected diffusion length¹¹ is $\sim 1000 \text{ \AA}$. At the surface S_0 interacts with a surface state whose energy E_t is located in the forbidden gap. The hole gets trapped, and if the trap level E_t is such that

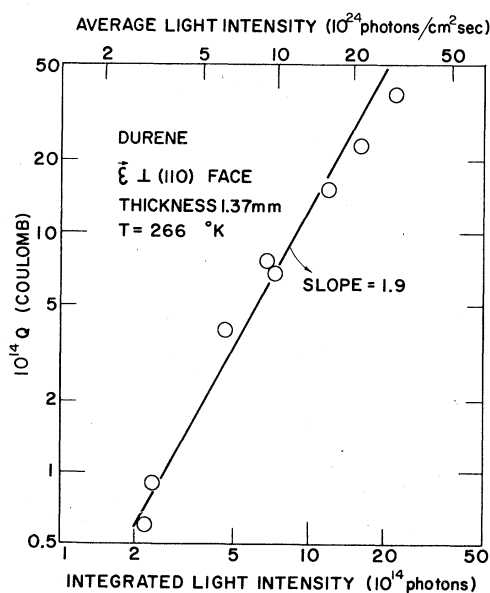


FIG. 5. Log-log plot of the collected charge for hole transients vs light intensity. The voltage across the crystal was 1800 V. Illuminated area $\sim 0.5 \text{ mm}^2$.

the energy $E_t + E_s$ is larger than the band-gap E_g , the electron becomes free. The electron still has to escape the Coulomb attraction of the trapped hole, given by $-e^2/\epsilon_r X$, where ϵ_r is the relative dielectric constant and X the distance measured from the trapped hole. The range of the Coulomb attraction, which is the distance at which the attractive energy becomes comparable to or smaller than the thermal energy $k_B T$, is about 200 \AA for room temperature. In view of the large mobilities in the a, b plane, the mean free path of the charge carriers should be of the same order of magnitude. The electron will thus diffuse out of the Coulomb attraction region (surface region) and be free to be swept by the external electric field. The hole trap level E_t (Fig. 6) is set just below the Fermi level at the surface. The actual position of the trap level could be anywhere up to several $k_B T$'s above the Fermi level to ensure that it is not already filled with a hole. To further simplify the figure it was assumed that the bands remain flat up to the contact, i.e., the Fermi level at the surface is at the middle of the gap. This, of course, is not necessarily the case. Surface states and contact potential are likely to cause band bending near the surface. The production of free holes can be envisioned through an analogous process involving electron traps.

Further insight into the charge-carrier generation process was obtained from a study of the voltage dependence of the amount of collected charge. In Fig. 7 some typical results for changes in the collected charge Q with applied voltage V are shown for hole transients at various temperatures. We first consider the voltage dependence. For very low temperatures (90 °K and 150 °K) the collected charge Q is proportional to $V^{1.5}$, while for the highest temperature shown it is directly proportional to V . An increase of the amount of col-

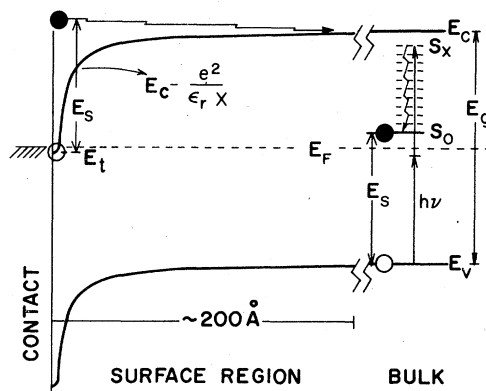


FIG. 6. A model suggested to explain the generation process of free electrons. For discussion see text.

lected charge with increasing voltage is an effect which has been observed in many similar studies on molecular crystals.^{19, 36-40}

One way to consider the voltage dependence is within Onsager's theory⁴¹ for geminate recombination of charge carriers. In this model the influence of the electric field is to enhance the dissociation of the charge carriers pair. The Q vs V plot⁴² would be linear with nonzero positive interception at $V=0$. Experimentally, this would be possible for "virgin" surfaces,⁴² where the surface recombination velocity is very small. For durene, however, all linear Q vs V plots for temperatures above ~ 150 K intercept at the origin, indicating that surface recombination is considerable.

Weisz *et al.*⁴³ consider that a voltage effect such as observed can be due to very high carrier trapping and/or recombination in a narrow region near the surface, the "electrode region." In the electrode region carriers of both types are present, and carrier recombination as well as trapping is possible; in the bulk only trapping is likely. When the carrier average lifetime at the electrode region τ_s is much shorter than the transit time across this region, a certain fraction of carriers will have recombined before reaching the bulk. The transit time in the electrode region is inverse-

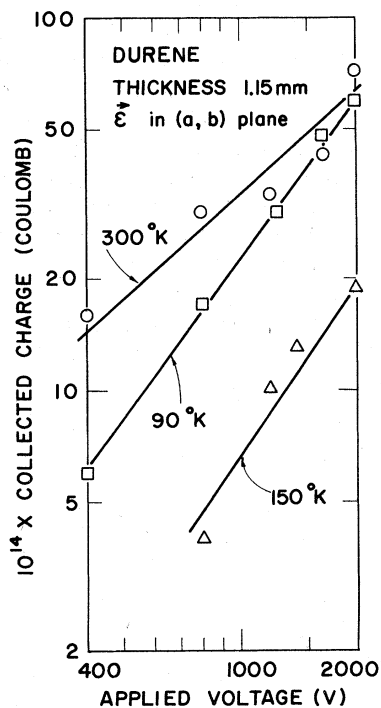


FIG. 7. Log-log plots of collected charge for hole transients vs voltage for various temperatures. Illuminated area ~ 1.5 mm². Integrated light intensity for each light pulse $\sim 2 \times 10^{15}$ photons. Electric field direction in a, b plane 45° between a and b .

ly proportional to the applied voltage, hence, the number of carriers that reach into the bulk of the crystal will increase with increasing voltage. Weisz *et al.*⁴³ predicted a linear dependence of the collected charge on the applied voltage by identifying the surface layer in which the carriers are generated with the layer of high recombination and/or trapping rates. The width of the electrode region is determined either by diffusion or by the penetration depth of surface traps into the bulk—whichever is the larger. The relation between Q and V predicted by this model is [see Eq. (36) in Ref. 43]

$$Q \approx \rho(0)\tau_s \mu A V L^{-1} e^{-2}, \quad (3)$$

where $\rho(0)$ is the volume density of the free charge carriers at the surface during the generation and A is the illuminated area. In the very general case τ_s could depend on the light intensity, the applied field and on the temperature. For applied voltages which are sufficiently high, the transit time across the electrode region becomes short compared to the trapping time. All carriers then enter the crystal bulk and are collected so the collected charge should saturate.¹⁹ Unfortunately, we could not reach saturation with our samples due to electrical breakdown.

Before analyzing our results in a similar manner to Weisz *et al.*,⁴³ we should carefully consider some of their simplifying assumptions. First suppose that the width of the electrode region d is indeed determined by the diffusion of the free charge carriers. That means that $d \approx \sqrt{D\tau_s}$, where the diffusion constant D is given by the Einstein relation $D = (k_B T/e)\mu$. Since the model implies that τ_s is much shorter than the transit time across the electrode region $\tau_0 (=Ld/\mu V)$, it follows that

$$d \ll \sqrt{D\tau_0}. \quad (4)$$

Inserting the Einstein relation and the expression for τ_0 into Eq. (4) gives

$$d \ll (k_B T/eV)L. \quad (5)$$

Some typical experimental parameters, $L \sim 1$ mm and $V = 2 \times 10^3$ V, give $d \ll 125$ Å at room temperature. This implies that the electrode region is confined within the Coulomb attraction range (see Fig. 6), but in this case the concept of transit time is meaningless. The second possibility to be considered is that the width of the electrode region is determined by the penetration depth of surface imperfections and impurities (which give rise to trapping states in the forbidden band). In order to estimate the width of the electrode region we take 100 – 200 Å as a lower limit for the diffusion length l . This is approximately the scattering length of charge carriers in view of their high mobility in the a, b plane. It can be easily shown that the con-

dition $\tau_0 \gg \tau_s$ implies that

$$d \gg (l^2/L)(eV/k_B T), \quad (6)$$

or $d \gg 100\text{--}200 \text{ \AA}$ at room temperature. For $\tau_0/\tau_s \sim 10$, $1000\text{--}2000 \text{ \AA}$ would be a lower limit for d , which is reasonable for the mechanically disturbed surface region.

Our data on the light intensity dependence of the collected charge (Fig. 5) suggest that in the electrode region, trapping rather than direct recombination, plays a dominant role. If recombination prevailed, the deviation from a perfect square law would have been more significant. This fact, together with the estimate of the width of the electrode region can provide an upper limit for the average density of free holes in the electrode region, if the hole-electron recombination rate constant K is known.

A fairly good estimate of K is given by Langevin's formula⁴⁴

$$K = 4\pi(e\bar{\mu}/\epsilon_r), \quad (7)$$

where $\bar{\mu}$ is the average relative mobility of holes and electrons. If the electron with which the hole is bound to recombine is trapped, the relative mobility is reduced to that of the free hole. Mobility anisotropy has also been excluded. Equation (7) is derived assuming that the charge-carrier mean-free path is short compared to the mutual electron-hole Coulomb attraction range (see Fig. 6). For durene, both values should be comparable in view of the high mobilities for the charge carriers in the a, b plane. This will reduce the recombination rate constant as charge carriers within the Coulomb attraction range can still escape recombination. Nevertheless, Eq. (7) should give an estimate for K correct to a factor of ~ 3 . For room temperature, taking $\bar{\mu} = 5 \text{ cm}^2/\text{V sec}$ we find $K \sim 3 \times 10^{-6} \text{ cm}^3 \text{ sec}^{-1}$. As mentioned, the slight sensitivity of τ_s to the light intensity implies that the recombination time τ_R should be long compared to the transit time of holes across the electrode region. The latter is of the order of 10^{-10} sec for a voltage of 2000 V. Since $\tau_R = 1/Kn$, where n is the density of electrons (free and trapped) we find that $n < 3 \times 10^{15} \text{ cm}^{-3}$. Assuming charge neutrality, $3 \times 10^{15} \text{ cm}^{-3}$ is an upper limit for the density of both free holes and electrons. Moreover, Eq. (3) enables us to determine a lower limit for the density of free holes. With an upper limit of 10^{-10} sec for τ_s , and the room temperature data of Fig. 7, one gets a value of $\sim 3 \times 10^{14} \text{ cm}^{-3}$ as the lower limit for $n(0) = \rho(0)/e$. We thus conclude that at room temperature, for an average light intensity of $\sim 5 \times 10^{25} \text{ photons/cm}^2 \text{ sec}$, the density of free holes at the electrode region during illumination is of the order of 10^{15} cm^{-3} .

This estimate of $n(0)$ will provide us, in addi-

tion, with an estimate of the rate constant for the singlet-singlet two photon absorption process. For simplicity, and since only an order-of-magnitude estimate is expected, we assume the following. (a) Only singlet excitons generated within the electrode region interact to produce free charge carriers. This is reasonable, for the estimate of the electrode region width (see above) is of the order of the expected singlet diffusion length or even larger. (b) All excited singlet excitons within the electrode region interact with the surface states before having a chance to decay via any other process. The quenching of singlet excitons at surface states is well known in other organic crystals.¹¹ This assumption (b) implies that the actual lifetime of the singlet excitons within the electrode region is much shorter than $\sim 30 \text{ nsec}$, the singlet radiative lifetime of durene in hexane.⁴⁵

Since the charge carrier lifetime in the electrode region ($10^{-11}\text{--}10^{-10} \text{ sec}$) is much shorter than the duration of the light pulse (10^{-8} sec), steady-state conditions are established and the density of free carriers at the surface $n(0)$ can be approximated by

$$n(0) \approx \alpha \sigma F^2 \tau_s = N \alpha \delta F^2 \tau_s, \quad (8)$$

where N is the density of molecules in the crystal, $0 < \alpha < 1$ is the fraction of the singlet-trap interactions which ultimately result in the liberation of the charge carrier, σ is the crystal singlet-singlet two-photon absorption rate constant, δ is the corresponding molecular rate constant, and F is the photon flux density (in units of photons $\text{cm}^{-2} \text{ sec}^{-1}$). Taking $F \sim 5 \times 10^{25} \text{ photons/cm}^2 \text{ sec}$, $\tau_s \sim 10^{-10} \text{ sec}$ and $N = 4.6 \times 10^{21} \text{ cm}^{-3}$ we find $\alpha \sigma \sim 5 \times 10^{-27} \text{ cm sec}$, $\alpha \delta \sim 10^{-48} \text{ cm}^4 \text{ sec}/(\text{photon molecule})$. These values should be regarded as lower limits for σ and δ since we took for τ_s the upper-limit value, and α is likely to be much smaller than unity (though larger than for anthracene in view of the larger mobilities). Calculated and measured values for two-photon absorption rate constants for anthracene and naphthalene from optical measurements are smaller than those estimated here.⁴⁶

The effect of temperature on the collected charge shows some interesting features. Between $300\text{--}150 \text{ }^\circ\text{K}$ the Q vs V plots are more or less linear, while for $150 \text{ }^\circ\text{K}$ and lower temperatures they tend to be superlinear. (See Fig. 7.) In the high-temperature range the measured integrated charge starts to increase again. Equation (3) suggests that a plot of the ratio Q/μ vs temperature should reflect the variation of the product $\rho(0)\tau_s$ with temperature. This ratio Q/μ is shown in Fig. 8 as a function of $1000/T$ for a constant field. The data shown include those from Fig. 7 for 2000 V,

together with additional results for both holes and electrons. The hole mobility for $T = 90^\circ\text{K}$ was estimated as $\sim 100\text{ cm}^2/\text{V sec}$ by extrapolation from the mobility data in Fig. 3, for at this temperature the transit time was too short to be reliably resolved. At higher temperatures Q/μ for both holes and electrons decreases with temperature with what appears to be an activation energy of about $\approx 0.1\text{ eV}$. Below about 150°K the curve seems to flatten, though few experimental points were determined for this range.

The trapping time in the electrode region τ_s is not expected to vary strongly with temperature. We therefore attribute the temperature dependence of Q/μ to that of $\rho(0)$. Then for the high-temperature range $\rho(0)$ is thermally activated with an activation energy of about $\sim 0.1\text{ eV}$. Several mechanisms can be envisioned which would account for this behavior. For example, it could mean that the energy location of the dominant sets of traps which interact with the singlet excitons to produce either free holes or free electrons is such that an additional energy of about $\sim 0.1\text{ eV}$ is required for the liberation of the free charge carrier. The flattening of the curve of Fig. 7 below $\sim 150^\circ\text{K}$ could be due to a contribution of another set of traps, which is located higher in energy so that its contribution is virtually independent of temperature. It is also possible that the two-photon process takes place both from the ground state and from a vibrationally excited ground state. The activation energy observed would then correspond to the Boltzmann population of this vibrational level and indeed durene exhibits a prominent vibration of $\sim 0.1\text{ eV}$ in its ground state.⁴⁷ In this case one would expect the activation energy for both holes and electrons to be the same, as is observed experimentally. Yet another effect to be considered is the temperature dependence of the electron-hole dissociation process itself. Following Onsager's theory it has been estimated⁴² that the dissociation process is thermally activated, with an activation energy [see Ref. 42, Eq. (15)] $E_a = e^2/\epsilon_r r_0$, where r_0 is the distance from the opposite-sign charged center, at which the free charge carrier thermalizes. For an activation energy of $\approx 0.1\text{ eV}$, as obtained for the high-temperature range (Fig. 8), r_0 should be about 50 \AA . Although this figure seems to be rather small to account for the high mobilities of durene, it cannot be ruled out. The flattening of the curve at low temperatures would then mean a fast increase in r_0 , which is not unreasonable since the mobility also increases. However more work is needed on durene to elucidate which of the possible mechanisms stated actually takes place. It should be noted, however, that at very low temperatures

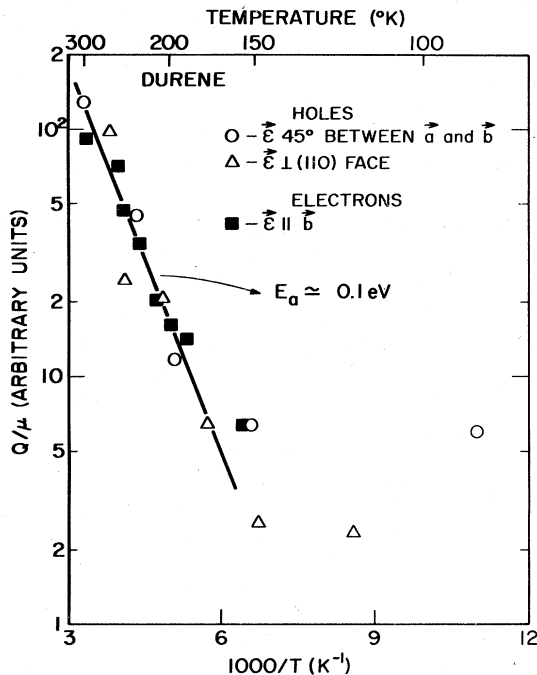


FIG. 8. Semilog plot of the ratio Q/μ vs $1000/T$ for both holes and electrons.

such as 90°K , for applied voltages of the order of 1000 V , the hole transit time across the electrode region is so short (10^{-11} – 10^{-10} sec) that one would expect it to become shorter than the hole trapping time. Then one would expect to observe a saturation of the collected charge, which was not found. On the contrary, in the low-temperature region one finds a superlinear voltage dependence (see Fig. 7). Presumably of greater importance is the effect of the voltage in increasing the carrier liberation rate⁴² by reducing the range of the Coulomb attraction (Fig. 6). The actual shape of the Coulomb attraction in the presence of an external field is slightly different from that shown in Fig. 6. The bands assume a maximum value, at a distance $X_m = e/\epsilon_r \mathcal{E}$ along the direction of the field. For a voltage of $\sim 1000\text{ V}$, X_m is about 200 \AA , and as the voltage increases, X_m decreases, thus increasing the probability of the charge carrier to escape the Coulomb attraction. It appears that the hole mean free path below $\sim 150^\circ\text{K}$ is such that the effect of the field is apparent only for this range. Thus one can rationalize the low-temperature voltage behavior (Fig. 7), in terms of the band diagram shown in Fig. 6, however no unequivocal evidence for the validity of this description could be derived from our data.

IV. CONCLUSIONS

Charge-carrier transport in molecular crystals is generally described by either of two limiting

cases, a band model or a localized polaron model. Which model is applicable depends upon the nature of the electron-phonon coupling, whether the dominant coupling is with inter- or intramolecular vibrations, if this coupling has a linear or quadratic dependence on the phonon coordinates, and of course the magnitude of the electron-phonon coupling compared to intermolecular exchange interactions.

In general drift mobilities for aromatic hydrocarbons fall in the range 1–3 cm²/Vsec, uncomfortably close to the theoretical lower limiting mobility for the applicability of a band model to these materials. Thus the observed carrier mobilities for durene in the crystal *a, b* plane (5 and 8 cm²/Vsec for holes and electrons respectively) are exceptional for this class of compound. The anisotropy of the measured mobilities (holes in the *c'* direction, $\mu = 0.15$ cm²/Vsec) can be fairly well explained in terms of the molecular crystal packing if we assume that mobilities will be smaller in the direction where electronic overlap is smaller. These high mobilities together with their temperature dependence, $T^{-2.5}$ in the *a, b* plane and $T^{-2.8}$ in the *c'* direction, indicate that in durene

carrier motion can be treated in terms of the band model.

The generation of charge carriers in organic materials is a complex process, particularly when light of lower photon energy than the first electronic transition is used. However, surface generation of charge carriers from singlet-excited states, themselves produced either in the bulk or on the surface, is very often the most important charge-carrier generation process. This has been found to be true for durene under the experimental conditions we have used. Little work has been reported in which the temperature dependence of charge-carrier generation in organics has been studied. In durene we have found an activation energy of ≈ 0.1 eV for both hole and electron generation in the range 150–300 K, but more work in durene and other crystals has to be performed before this behavior can be fully understood.

ACKNOWLEDGMENTS

We are indebted to Dr. A. W. Hanson for the crystallographic alignment of our samples.

- ¹A. Szent-Györgi, *Science* **93**, 609 (1941).
- ²See, for example, L. B. Coleman, M. J. Cohen, D. J. Sandman, F. G. Yamagishi, A. F. Garito, and A. J. Heeger, *Solid State Commun.* **12**, 1125 (1973).
- ³O. H. LeBlanc, Jr., *J. Chem. Phys.* **35**, 1275 (1961).
- ⁴R. W. Munn and W. Siebrand, *J. Chem. Phys.* **52**, 47 (1970).
- ⁵P. Gossar and S. L. Choi, *Phys. Rev.* **150**, 529 (1966).
- ⁶K. F. Herzfeld, *Chem. Rev.* **41**, 233 (1947).
- ⁷D. Leonard, *Appl. Phys. Lett.* **7**, 4 (1965).
- ⁸J. Tanaka, *Bull. Chem. Soc. Jpn.* **36**, 833 (1963).
- ⁹R. G. Kepler, *Phys. Rev.* **119**, 1226 (1960).
- ¹⁰J. M. Robertson, *Proc. R. Soc. A* **141**, 594 (1933).
- ¹¹O. H. LeBlanc, Jr., in *Physics and Chemistry of the Organic Solid State*, edited by D. Fox, M. M. Labes, and A. Weissberger (Interscience, New York, 1967), Vol. III, p. 133.
- ¹²Y. Maruyama, T. Kobayashi, and H. Inokuchi, *Mol. Cryst. Liq. Cryst.* **20**, 373 (1973).
- ¹³C. E. Swenberg, D. Markevich, N. E. Giacintov, and M. Pope, *Phys. Status Solidi A* **29**, 651 (1975).
- ¹⁴H. Möhwald and D. Haarer, *Mol. Cryst. Liq. Cryst.* **32**, 215 (1976).
- ¹⁵Z. Zboinski, *Mol. Cryst. Liq. Cryst.* **32**, 219 (1976).
- ¹⁶T. J. Sonnonstine, A. Winglesworth, and A. M. Hermann, *J. Chem. Phys.* **59**, 3865 (1973).
- ¹⁷G. A. Cox and P. C. Knight, *Phys. Status Solidi B* **50**, K135 (1972).
- ¹⁸H. Hirth and F. Stöckmann, *Phys. Status Solidi B* **51**, 691 (1972).
- ¹⁹Y. Aoyagi, K. Masuda, and S. Namba, *Mol. Cryst. Liq. Cryst.* **22**, 301 (1973).
- ²⁰J. Kondrasiuk and A. Szymanski, *Mol. Cryst. Liq. Cryst.* **18**, 379 (1972).
- ²¹P. Di Marco and G. Giro, *Mol. Cryst. Liq. Cryst.* **29**, 179 (1975).
- ²²W. G. Williams, *Discuss. Faraday Soc.* **51**, 61 (1971).
- ²³L. M. Schwartz, H. G. Ingersol, Jr., and J. F. Hornig, *Mol. Cryst. Liq. Cryst.* **2**, 379 (1967).
- ²⁴For a discussion see, C. K. Ingold, *Structure and Mechanism in Organic Chemistry*, 2nd ed. (Cornell U.P., Ithaca, 1969), Chaps. 3 and 5.
- ²⁵W. E. Spear, *Crit. Rev. Solid State* **3**, 523 (1974).
- ²⁶S. H. Glarum, *Phys. Chem. Solids* **24**, 1577 (1965).
- ²⁷L. Friedman, *Phys. Rev.* **140**, A1649 (1965).
- ²⁸H. Fröhlich and G. L. Sewell, *Proc. Phys. Soc. Lond.* **74**, 643 (1959).
- ²⁹R. W. Munn and W. Siebrand, *J. Chem. Phys.* **52**, 6391 (1970).
- ³⁰R. G. Kepler, in *Phonons and Phonon Interactions*, edited by T. A. Bak (Benjamin, New York, 1964), p. 578.
- ³¹R. Mason, *Acta Crystallogr.* **17**, 547 (1964).
- ³²A. Handi, B. Wyneke, G. Morlot, and X. Gerbaux, *J. Chem. Phys.* **51**, 3514 (1969).
- ³³H. Sponer and Y. Kanda, *J. Chem. Phys.* **40**, 778 (1964).
- ³⁴P. Avakian and R. E. Merrifield, *Mol. Cryst. Liq. Cryst.* **5**, 37 (1968).
- ³⁵This crude estimate was made in the spirit of L. E. Lyons, in *Physics and Chemistry of the Organic Solid State*, edited by D. Fox, M. M. Labes, and A. Weissberger (Interscience, New York, 1963), Vol.

- I, pp. 759-775.
- ³⁶A. Many, M. Simhony, S. Z. Weisz, and J. Levinson, *J. Phys. Chem. Solids* 22, 285 (1961).
- ³⁷A. Many, S. Z. Weisz, and M. Simhony, *Phys. Rev.* 126, 1989 (1962).
- ³⁸W. Helfrich and P. Mark, *Z. Phys.* 166, 370 (1962).
- ³⁹M. Silver *et al.*, *J. Phys. Chem. Solids* 23, 419 (1963).
- ⁴⁰C. Bogus, *Z. Phys.* 184, 219 (1965).
- ⁴¹L. Onsager, *Phys. Rev.* 54, 554 (1938).
- ⁴²R. R. Chance and C. L. Braun, *J. Chem. Phys.* 64, 3573 (1976).
- ⁴³S. Z. Weisz, A. Cobas, S. Trester, and A. Many, *J. Appl. Phys.* 39, 2296 (1968).
- ⁴⁴W. Helfrich, in *Physics and Chemistry of the Organic Solid State*, edited by D. Fox, M. M. Labes, and A. Weissberger (Interscience, New York, 1967) Vol. III, p. 1.
- ⁴⁵P. M. Fröhlich and H. A. Morrison, *J. Phys. Chem.* 76, 3566 (1972).
- ⁴⁶R. Pantell, J. Hanus, M. Schott, and H. Puthoff, *J. Chem. Phys.* 46, 3507 (1967).
- ⁴⁷M. Martin-Bouyer, *J. Chim. Phys.* 64, 1621 (1967).